Transport of Organic Components from Immobile and Bypassed Oil in Porous Media

O. Huseby, A. Haugan, J. Sagen, and J. Muller
Institutt for Energiteknikk, Kjeller, Norway

B. Bennett and S. Larter
NRG, Drummond Building, University of Newcastle, Newcastle upon Tyne, UK

E. S. Kikkinides
CPERI, Center for Research and Technology Hellas, Thessaloniki, Greece

A. K. Stubos
National Center for Scientific Research–Demokritos, Athens, Greece

F. Yousefian and J.-F. Thovert
Laboratoire de Combustion et de Détonique, Poitiers, France

P. M. Adler
Institut de Physique du Globe de Paris, Paris, France

An experimental study, as well as theoretical and numerical models, are used to validate a methodology to exploit conventional geochemical data with regard to the concentration profiles of organic components occurring naturally in hydrocarbon reservoir oils. The experiment was designed to study transport of organic compounds from bypassed oil during water injection using a homogeneous oil-filled core sample, which was made heterogeneous by drilling a hole through its central axis and filling it with a highly permeable material. Under the present conditions, diffusion coefficients are the most important parameters controlling the transport, and the effect of partitioning could be accounted for by a simple normalization. The experimental results are well described by a simple 2-D analytical model that assumes instantaneous removal of solutes from the oil–water interface. The experimental results are also well described by two numerical models, of which one is a full-featured reservoir scale model, suitable for applications of the methodology to reservoir-scale cases.

Introduction

The task of estimating the presence and location of bypassed oil is highly relevant to tertiary oil recovery methodologies. Such methodologies are expected to become more important as the discovery of new oil reserves starts to decline. In 1996, for example, about 3% of the world's oil production and about 11% of the U.S. production came from enhanced oil recovery (EOR) projects (Taber et al., 1997).

The obvious economic potential represented by undeveloped oil in existing oil reservoirs is therefore an important motivation for studies related to the estimation and production of bypassed oil. Undeveloped oil from bypassed regions in mature oil fields is discussed by, for example, Watters et al. (1999), Montgomery et al. (1998), and Walker (1997). Experimental studies of mass transfer from bypassed oil have been conducted by Le Romancer et al. (1994), Burger et al. (1996), and Burger and Mohanty (1997).

In addition to the relevance for oil production, the estimation of the presence and location of oil pools is also relevant in subsurface hydrology. Increasing attention has been devoted to the estimation of the presence of nonaqueous phase liquids (NAPLs) and remediation of NAPL contaminated

Correspondence concerning this article should be addressed to O. Huseby.

groundwater resources. In a recent review of this topic, Khachikian and Harmon (2000) mention the lack of efficient NAPL location methodologies as one of the obstacles that precludes effective deployment of NAPL recovery technologies.

Use of injected partitioning tracers is one of the techniques employed to estimate the presence of undeveloped oil or NAPL contamination. In the context of hydrocarbon reservoirs, this is demonstrated by Lichtenberger (1991). In subsurface hydrology, this technique is demonstrated by Jin et al. (1995).

Complementary information on undeveloped oil or NAPL contamination, compared to that generated by the injection of partitioning tracers, can be obtained from the presence (or absence) of chemical compounds in fluids produced from subsurface water or hydrocarbon reservoirs. In the case of subsurface hydrology, Semprini et al. (2000) describe a methodology based on the reduction of radon-222 concentration as an estimation and quantification tool for NAPL contamination.

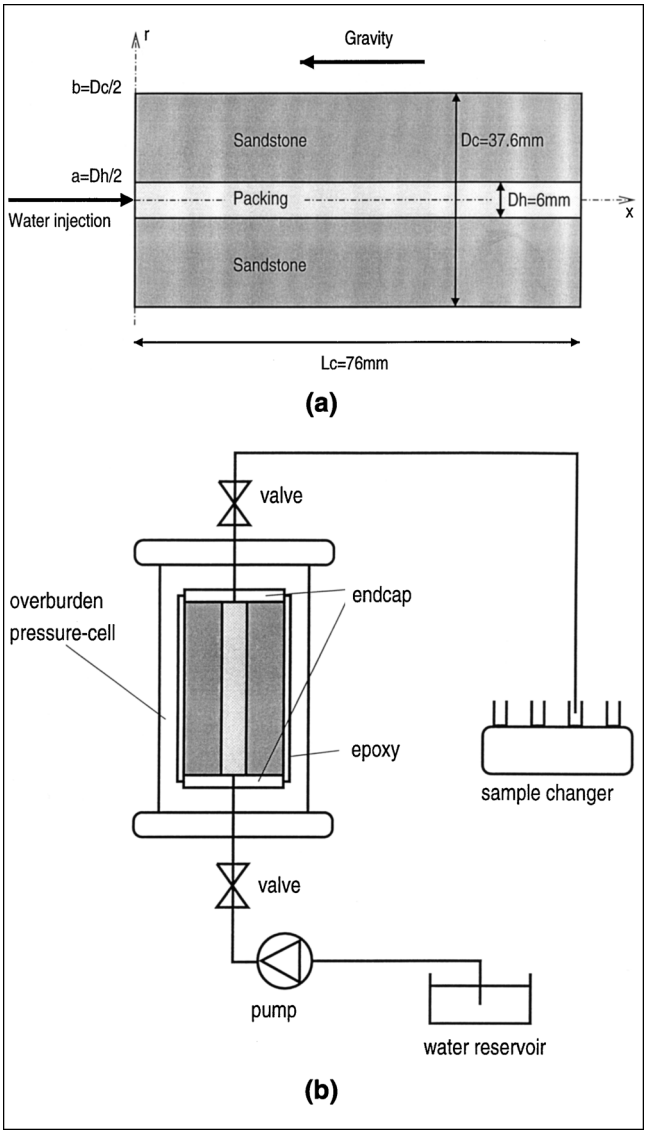

Figure 1. Geometry (a) and rig lay-out (b) of the experimental case.

Presently, we suggest a methodology that exploits conventional geochemical data with regard to the concentration profiles of organic components occurring naturally in hydrocarbon reservoir oils. To validate the methodology, a laboratory experiment was performed, accompanied by theoretical and numerical models for the production profiles of these "natural tracers" in a hydrocarbon reservoir.

The experiment was designed to mimic the bypassing of oil occurring in heterogeneous reservoirs due to permeability variations and nonoptimal location of injection or production wells. A homogeneous cylindrical core sample from a North Sea field was transformed to a heterogeneous one by drilling a hole along its central axis and filling it with a highly permeable porous material, through which fluids are allowed to pass.

The present experiment bears similarities to tests conducted by Le Romancer et al. (1994), Burger et al. (1996), and Burger and Mohanty (1997). However, whereas these authors were concerned with the transport of oil from the low permeability areas during gas injection, our objective is to study transport of organic compounds from the immobile oil during water injection. In our case, the oil is kept immobile due to the small permeability of the core material.

To the best of our knowledge, no such experimental or theoretical studies exist on the production of oil components from immobile bypassed oil during water injection.

The rest of this article is organized as follows: First the experimental setup and procedure are described, and physical properties of the fluids and the geometry are determined, including the transport coefficients of the porous materials. Then the transport equations and two models are presented and an analytical treatment of the problem is given, as well as a brief description of numerical codes used to model the experiment. The experimental results are presented and compared to the numerical and theoretical models. Finally, the main findings are briefly summarized in the last section.

Experiment

Experimental setup and procedure

A cylindrical sample of a reservoir sandstone from the North Sea was prepared and perforated by drilling a cylindrical hole along its central axis, as shown in Figure 1a.

The experiment was carried out in a small-core flow rig, illustrated in Figure 1b. The core was coated with epoxy, and two stainless steel endcaps were connected to the circular ends of the core. The endcaps have a special broken ring-shaped pattern toward the core, in order to distribute the entrance liquid across the entire entrance cross section, and, similarly, to collect the exit fluid from the entire exit cross section. The liquid flow is supplied through 3.175 mm (1/8 in.) stainless steel tubing using an HPLC pump (Beckman 114M). The space between the hole and the valves was covered by a reticulate wire, in order to avoid the plastic spheres escaping from the central hole. The complete core, with coating and endcaps, was placed in a Hassler cell, and an overburden pressure of 10 bar was applied to avoid cracking the

epoxy coating. The exit fluid was directed to a sample collector (Gilson Model 222) and stored in test tubes for later concentration measurements. The methodology used to find the solute concentrations is described below.

Initially, the rock was dried to remove any water from the sandstone. Air was removed from the sample, and the whole sample (including spherical packing and tubing) was completely saturated with oil from a specific well (Well-A3) in the Veslefrikk field in the North Sea. The experiment was performed by injecting synthetic formation water at the inlet and pumping it through the system. Note that the inlet is located at the bottom of the sample, which is important in order to remove the oil from the central packing, since the oil is less dense than water. For a transient period of about 2 h, the oil originally located in the packing and tubing was produced. Afterwards, the experiment was continued for 90 h, measured from the time of water breakthrough. The experiment was carried out at room temperature ($T = 20$°C). During the experiment, the outlet was kept at atmospheric pressure $P_o = 10^5$ Pa, and water was injected at the inlet at a constant flow rate $Q = 1.044\ 10^{-6}$ m^3/h. The produced water was sampled every hour during the experiment. Samples of the produced water were analyzed and concentrations of phenol, orthocresol, paracresol, and metacresol in the produced water recorded as explained below.

Geometrical, fluid, and transport properties

Geometrical Properties. The length of the sample is $L_c = 76$ mm, its radius $b = 18.8$ mm, and the hole radius $a = 3.0$ mm. The cylindrical hole was filled with spherical plastic particles of diameter $d = 0.5$ mm.

The porosity of the sandstone was measured and is $\epsilon_s = 0.193$. The porosity of the sphere packing $\epsilon_p = 0.397$ was estimated by using the results of experiments and numerical simulations of bead deposition (Scott, 1960; Berryman, 1983; Coelho et al., 1997).

Initially the water saturation in the sample was zero, as the sample was completely saturated with oil after washing.

Fluid and Solute Properties. The viscosity of the oil was measured at room temperature (22.6°C), using a viscosimeter (Physica Viscolab LC100). Its value is $\mu_o = 9.6 \pm 0.3$ cP.

The oil contains phenol, *o*-cresol, *p*-cresol, and *m*-cresol, which are the naturally occurring organic solutes used in this study. Their initial concentrations were measured and found equal to 3.9 mg/L, 6.3 mg/L, 1.8 mg/L, and 2.1 mg/L for phenol, *o*-cresol, *p*-cresol, and *m*-cresol, respectively.

The composition of the injected water was estimated based on measurements of the formation water from Well-A3 in the Veselfrikk field in the North Sea. The analysis shows the following chemical compounds (all quantities in g/L): NaCl 36.855, KCl 0.629, $CaCl_2 \cdot 2H_2O$ 3.814, $MgCl_2 \cdot 6H_2O$ 2.550, $BaCl_2 \cdot 2H_2O$ 0.088, $SrCl_2 \cdot 6H_2O$ 0.437, $NaHCO_3$ 0.207, Na_2SO_4 0.046.

Partition coefficients are given as $k = C_o^{\mathrm{eq}}/C_w^{\mathrm{eq}}$, where C_o^{eq} and C_w^{eq} are concentrations under equilibrium conditions in the oil and water phases, respectively (Bennett and Larter, 1997). They were measured for salinity values 5% and 15%, at 50°C and 100°C, and partition coefficients for salinity 3.7% and temperature 20°C were estimated by a linear extrapolation. They are

$$k = 0.3\ (\text{phenol}) \qquad k = 2.1\ (m\text{-cresol}),$$
$$k = 3.8\ (o\text{-cresol}), \qquad k = 2.3\ (p\text{-cresol}). \tag{1}$$

Adsorption of the solutes onto the rock surface was not measured directly, but the thin sections suggest that the rock consists mainly of quartz. Adsorption in sandpacks made from similar sand from the same reservoir rock was investigated and found to be negligible. Addition of 1.16% kerogen to the sandpacks, on the other hand, seriously altered the sorption behavior.

Diffusion and Dispersion Properties. The molecular diffusion coefficients $D_{m,w}$ and $D_{m,o}$ of the organic solutes in water and oil were estimated using the Wilke–Chang and Hayduk–Mindas expressions, respectively (Perry et al., 1997). The variations of $D_{m,w}$ and $D_{m,o}$ for the various solutes are less than the ~20% error of the Wilke–Chang and Hayduk–Mindas correlations, therefore, the average values for the molecular diffusion coefficients $D_{m,o} = 3.8 \times 10^{-10}$ m^2/s and $D_{m,w} = 7.8 \times 10^{-10}$ m^2/s are used in the following.

The effective diffusion coefficient in the sandstone is $D_{m,o}/(F_s \epsilon_s)$, where F_s, the formation factor, is the inverse of the dimensionless electrical conductivity $1/F_s = \sigma/\sigma_0$ of a porous medium saturated with a conducting liquid of conductivity σ_0. The conductivity coefficient $1/F_s = 0.0132 \pm 0.0008$ was computed by solving the Laplace equation in three-dimensional numerical samples reconstructed according to the statistical geometrical properties measured on thin sections, as described in Adler (1992).

The longitudinal and transversal dispersion coefficients depend on the Péclet number $Pe = v_p^* d/D_{m,w}$, where v_p^* is the mean interstitial velocity. They are well described by power laws in the Péclet number range $\sim 5 < Pe < \sim 300$ (Pfannkuch, 1963; Bear, 1972)

$$D_{p\|}^* = \beta_{\|} Pe^{\alpha\|}, \qquad D_{p\perp}^* = \beta_{\perp} Pe^{\alpha\perp} \tag{2}$$

A least-square fit of the results of Coelho et al. (1997) for spherical grain packings yields

$$\alpha_{\|} = 1.25, \qquad \beta_{\|} = 0.0984 \tag{3}$$
$$\alpha_{\perp} = 0.698, \qquad \beta_{\perp} = 0.166. \tag{4}$$

With a flow rate $Q = 1.044$ mL/h, this gives

$$v_p^* = \frac{Q}{\pi a^2 \epsilon_p} = 25.8\ 10^{-6}\ \text{m/s}, \qquad Pe = \frac{v_p^* d}{D_{m,w}} = 16.5,$$
$$D_{p\|}^* = 3.27, \qquad D_{p\perp}^* = 1.17. \tag{5}$$

Finally a permeability simulation using the reconstructed sandstone sample was performed, which yields $K_s \approx 0.4$ Da for the sandstone, whereas Coelho et al. (1997) obtain $K_p \approx 110$ Da for the sphere packing.

Quantification of phenol and cresols

Phenol and cresols were isolated from the oil sample, by solid-phase extraction (SPE). The procedure is described in

detail elsewhere (Bennett et al., 1996). Briefly ca. 400 mg of oil is loaded onto a C18 nonendcapped cartridge (Isolute, Jones chromatography), interferents (including hydrocarbons) are eluted with 5 mL petroleum ether. Phenol and cresols are recovered in 5 mL 50:50 volume methanol:water, and subsequently diluted to an accurate volume, usually 10 mL. The SPE extract is analyzed by reverse-phase high-performance liquid chromatography with electrochemical detection (RP-HPLC-ED). The sampled fluids (aqueous), however, require little preparation and can be analyzed directly by RP-HPLC-ED.

A Hewlett-Packard HP 1050 was used. Sample injection (20 mL volume) was by autosampler. Detection was performed using an Antec Decade Electrochemical Detector (Presearch UK). The detector cell was equipped with a glassy carbon electrode and a silver/silver chloride reference electrode. The potential applied for phenol analysis was +0.6 V. HPLC conditions were adopted from Nieminen and Heikkila (1986). The mobile phase comprised 17% acetonitrile, 83% aqueous 0.1 M sodium acetate adjusted to pH 11.5–11.6 with 1 M NaOH. pH measurements were monitored with an ATC pH meter (Piccolo 2 by Hanna). The column was a Hamilton PRP-1 (150 mm×4.1 mm ID) with particle diameter 10 mm. Flow rate was 2 mL/min.

A standard stock solution of phenol and cresol used for quantification purposes was prepared in distilled/deionized water and stored in a refrigerator until required. Aliquots were taken from the stock solution and diluted to the levels expected in the samples. Standard solutions were prepared from the stock solution on a daily basis. A typical run sequence consisted of a standard, 2 samples; repeat standard, 2 samples, and so on. Quantification of phenol and cresol detected in standard solutions and samples were based on peak area measurements obtained using Multichrom (VG Lab System) running on a DEC MicroVax 3100.

The analysis of the produced fluids from the individual test tubes was performed in random order, to avoid possible analytical bias from sample ordering.

Modeling Approaches

Two models were used to analyze the problem, one that assumes immobile oil in the sandstone, which yields a one-phase flow problem, and one that allows for imbibition of water into the sandstone. Two numerical implementations were used; one of these is applicable to both of the models, whereas the other assumes a one-phase problem. The problem was also solved by an analytical approach to the one-phase model.

General

The solute conservation equation in the presence of oil and water is

$$\epsilon\frac{\partial}{\partial t}(S_w c + kS_o c) + \nabla\cdot(S_w\epsilon\boldsymbol{v}_w^* c + kS_o\epsilon\boldsymbol{v}_o^* c) - \nabla)(S_w\epsilon\boldsymbol{D}_w^* + kS_o\epsilon\boldsymbol{D}_o^*)\cdot\nabla c) = 0, \quad (6)$$

where $\boldsymbol{v}_i^* = \bar{\boldsymbol{v}}_i/\epsilon S_i$ are the fluid interstitial velocities. Here, instantaneous local equilibrium has been assumed, and oil phase concentration, c_o, can be related to water-phase concentration, $c_w \equiv c$, by

$$c_o = kc. \quad (7)$$

The velocities and saturations can be obtained from the solution of the two-phase flow problem (Aziz and Settari, 1979).

The boundary conditions follow from no flux at $r = b$ and injection of pure water at $x = 0$ for $r < a$

$$\boldsymbol{n}\cdot\nabla c = 0 \quad \text{for} \quad r = b, \qquad c = 0 \quad \text{for} \quad r < a, \qquad x = 0. \quad (8)$$

The initial conditions are

$$t = 0: \qquad c = \begin{cases} 0 & \text{if } r < a \\ c_0/k & \text{if } r \geq a, \end{cases} \quad (9)$$

where c_0 is the initial solute concentration in the oil.

The dispersion tensors $\boldsymbol{D}_i^*$ can be written as

$$\boldsymbol{D}_i^* = D_{m,i}\left\{D_{i\|}^*\boldsymbol{e}_\|\boldsymbol{e}_\| + D_{i\perp}^*\left(\boldsymbol{I} - \boldsymbol{e}_\|\boldsymbol{e}_\|\right)\right\}, \quad (10)$$

where i denotes oil or water, and $D_{m,i}$ is the solute molecular diffusion coefficient. The coefficients $D_{i\|}^*$ and $D_{i\perp}^*$ depend on the flow velocity of phase i through the Péclet number

$$Pe_i = \frac{v_i^* d}{D_{m,i}}. \quad (11)$$

Models

One-Phase Model. The experiment was designed in order to have stagnant oil in the sandstone and flowing water in the packing. A first idealized model was therefore formulated, with constant saturation functions for water and oil

$$S_w(r,x) = 1 - S_o(r,x) = \begin{cases} 0 & \text{if } r > a \\ 1 & \text{if } r \leq a. \end{cases} \quad (12)$$

In this model, the oil-phase velocity is assumed to be zero $\boldsymbol{v}_{o,s}^* = 0$ in the sandstone, whereas the water phase flows with a uniform interstitial velocity $\boldsymbol{v}_{w,p}^*$. This model was studied using a two-phase flow simulator, simply by setting the relative permeability to one and sandstone permeability to zero, and using Eqs. 6–9 directly.

Alternatively, the idealized model can be investigated using a one-phase code, using two one-phase equations, with an additional continuity condition on the solute fluxes on the sandstone–packing interface. This formulation is also useful to obtain an analytical solution to the problem, which will be given in the next section. With the assumption (Eq. 12), Eq. 6 takes simple forms in both the sandstone and the packing. In the sandstone, the zero oil velocity and $S_{o,s} = 1$ yields

$$\epsilon_s k\frac{\partial c}{\partial t} - k\nabla\cdot(\epsilon_s\boldsymbol{D}_{o,s}^*\cdot\nabla c) = 0. \quad (13)$$

Note that even if the water phase is absent, c is still defined, because $c_i = c_o = kc$. In the packing, where oil saturation is

zero and water flows with a constant velocity $\boldsymbol{v}^*_{w,p}$

$$\epsilon_p \frac{\partial c}{\partial t} + \nabla\cdot(\epsilon_p \boldsymbol{v}^*_{w,p} c) - \nabla\cdot(\epsilon_p \boldsymbol{D}^*_{w,p}\cdot\nabla c) = 0. \qquad (14)$$

Continuity of normal fluxes yields the additional boundary condition on the interface $r = a$

$$k\epsilon_s \boldsymbol{n}\cdot\boldsymbol{D}^*_{o,s}\cdot\nabla c = \epsilon_p \boldsymbol{n}\cdot\boldsymbol{D}^*_{w,p}\cdot\nabla c. \qquad (15)$$

In the absence of flow, $\boldsymbol{D}^*_{o,s}$ in the sandstone reduces to

$$\boldsymbol{D}^*_{o,s} = \frac{D_{m,o}}{F_s\epsilon_s}\boldsymbol{I}, \qquad (16)$$

where $D_{m,o}$ is the solute molecular diffusion coefficient in the oil, and F_s is the sandstone formation factor.

Imbibition Model. However, depending on the wettability of the sandstone, spontaneous imbibition is likely to have an effect, and some oil could be produced even after water breakthrough. Indeed, the measured concentrations could not be explained by diffusive transport alone, and suggest that about 6% of the oil in the sandstone was produced during the first 15 h of the experiment. To capture this effect, a second model was used, with linear relative permeability curves

$$K_{rw} = 1 - K_{ro} = \begin{cases} 5/4S_w - 1/8 & \text{if } 0.1 \le S_w \le 0.9 \\ 0 & \text{otherwise.} \end{cases} \qquad (17)$$

In addition, the permeability in the sandstone was arbitrarily set to $K_s = 5$ Da for $a < r < d = 0.55$ cm and $K_s = 10^{-5}$ Da for $d < r < b$. This value of d and the critical water saturation, $S_{wc} = 0.9$ ($K_{rw} = 0$ for $S_w > S_{wc}$), yields an amount of 0.93 cm^3 oil produced from the sandstone. This oil is produced from the volumes adjacent to the water flowing in the packing, which is consistent with the experiments by Bourbiaux and Kalaydjian (1990). With the choice $K_s = 5$ Da for $a < r < d$, 89% of this oil is produced within the first 5 h, 97% within 15 h, and 99.9% within 25 h. After about 25 h, the transport of solutes from the sandstone is almost purely diffusive.

This model was studied with the help of a two-phase simulator, and using Eqs. 6–9 directly.

Dimensionless Formulation. Dimensionless variables denoted by primes can be defined by using the characteristic quantities c_0/k, $D_{m,o}/(F_s\epsilon_s)$, and a

$$c' = kc/c_0 \qquad (18)$$

$$x' = \frac{x}{a}, \qquad r' = \frac{r}{a}, \quad \nabla' = a\nabla \qquad (19)$$

$$t' = \frac{D_{m,o}}{a^2 F_s\epsilon_s}t, \qquad \boldsymbol{D}^{*\prime}_i = \frac{F_s\epsilon_s}{D_{m,o}}\boldsymbol{D}^*_i, \qquad \boldsymbol{v}^{*\prime}_p = \frac{aF_s\epsilon_s}{D_{m,o}}\boldsymbol{v}^*_i. \qquad (20)$$

In dimensionless form, Eq. 6 and the boundary conditions (Eqs. 8) read

$$\epsilon\frac{\partial}{\partial t'}(S_w c' + kS_o c') + \nabla'\cdot(S_w\epsilon\boldsymbol{v}^{*\prime}_w c' + kS_o\epsilon\boldsymbol{v}^{*\prime}_o c') - \nabla'\cdot(S_w\epsilon\boldsymbol{D}^{*\prime}_w\cdot\nabla' c' + kS_o\epsilon\boldsymbol{D}^{*\prime}_o\cdot\nabla' c') = 0 \qquad (21)$$

$$\boldsymbol{n}\cdot\nabla' c' = 0 \quad \text{for} \quad r' = b', \qquad c' = 0 \quad \text{for} \quad r' < 1, \qquad x' = 0. \qquad (22)$$

The initial conditions (Eqs. 9) are

$$t' = 0: \qquad c' = \begin{cases} 0 & \text{if } r' < 1 \\ 1 & \text{if } r' \ge 1. \end{cases} \qquad (23)$$

Equations 13 and 14 read in dimensionless form

$$\frac{\partial c'}{\partial t'} - \nabla'^2 c' = 0 \qquad (24)$$

$$\frac{\partial c'}{\partial t'} + \nabla'\cdot(\boldsymbol{v}^{*\prime}_{w,p} c') - \nabla'\cdot(\boldsymbol{D}^{*\prime}_{w,p}\cdot\nabla' c') = 0, \qquad (25)$$

and the continuity condition on normal fluxes at $r' = 1$ (Eq. 15) yields

$$\boldsymbol{n}\cdot\nabla'_+ c' = \frac{\epsilon_p}{k\epsilon_s}\boldsymbol{n}\cdot\boldsymbol{D}^{*\prime}_{w,p}\cdot\nabla'_- c', \qquad (26)$$

where ∇_+ and ∇_- refer to the gradients on the outer and inner sides, respectively.

This dimensionless formulation shows that the system behavior is determined by a single dimensionless parameter, $\epsilon_p/k\epsilon_s$, in addition to the Péclet number Pe.

Analytical solution

The one-phase problem can be solved analytically, based on the assumption that the variations of c with x in the sandstone are negligible, since the solute is washed out at $r = a$. In other words

$$c = 0 \quad \text{at} \quad r = a. \qquad (27)$$

This assumption implies that the concentration field in the sandstone is governed by a one-dimensional equation. The problem (Eqs. 21–23) then reads

$$\frac{\partial c}{\partial t} - \left(\frac{\partial^2 c}{\partial r^2} + \frac{1}{r}\frac{\partial c}{\partial r}\right) = 0 \qquad \text{for} \quad 1 \le r \le b, \qquad (28)$$

with boundary conditions

$$c = 0 \quad \text{for} \quad r = 1 \qquad (29)$$

and

$$\frac{\partial c}{\partial r} = 0 \quad \text{for} \quad r = b, \qquad (30)$$

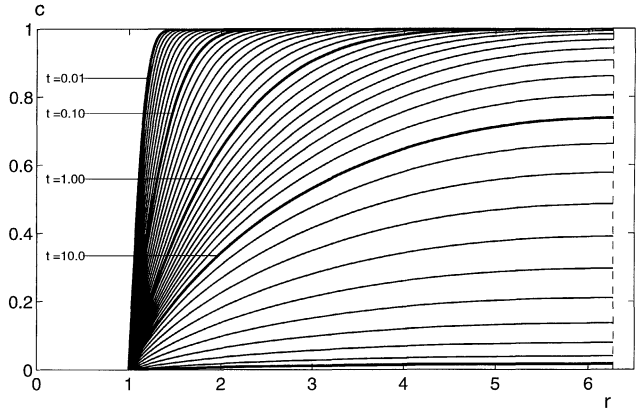

Figure 2. Analytical radial concentration profiles at various times, given by Eqs. 32–34.

and initial conditions

$$c = 1 \quad \text{for} \quad t = 0, \tag{31}$$

where the primes of the dimensionless variables have been removed to simplify the notations.

With the definition of the dimensionless time in Eq. 20 and of the quantities given in the experimental section, a unit dimensionless time corresponds to 346,290 s = 96.1 h, that is, roughly to the total duration of the physical experiment.

The solution to Eqs. 28–31 is classic (Carslaw and Jaeger, 1959)

$$c = -\sum_{n=1}^{\infty} C_n \left[J_0(r\alpha_n) Y_0(\alpha) - Y_0(r\alpha_n) J_0(\alpha) \right] e^{-\alpha_n^2 t}, \tag{32}$$

where

$$C_n = \pi \frac{J_1^2(b\alpha_n)}{J_0^2(\alpha_n) - J_1^2(b\alpha_n)} \tag{33}$$

and α_n are the solutions of the equation

$$J_0(\alpha) Y_1(b\alpha) - Y_0(\alpha) J_1(b\alpha) = 0. \tag{34}$$

Radial concentration profiles for increasing dimensionless times, 10^{-2} to 10^{+2}, are plotted in Figure 2 for the ratio $b/a = 6.2667$ in the real experiment.

The figure shows that the concentration depletion reaches the outer boundary, $r = b$, at a dimensionless time larger than unity, that is, not during the duration of the experiment. In other words, the sample diameter is large enough so that it behaves as an infinite medium, in the measurement time interval.

The amount $M(t)$ of solute remaining in the sandstone can be derived from Eq. 32. When normalized by the initial solute quantity $M_0 = M(0)$, it reads

$$\frac{M(t)}{M_0} = \frac{2}{b^2 - 1} \int_1^b rc(r)\, dr. \tag{35}$$

The solute flux J emitted per unit length to the central channel can be derived by either of the two expressions

$$J = -2\pi\epsilon_s \left(\frac{\partial c}{\partial r} \right)_{r=1} = -\frac{dM}{dt}. \tag{36}$$

For early times, J is well described by a power-law fit

$$J \approx t^{-0.430} \qquad (t \le 0.3). \tag{37}$$

After this initial period and before M has significantly decreased ($M \ge M_0/2$), another exponent applies

$$J \approx 1.19 t^{-0.301} \qquad (0.3 \le t \le 10). \tag{38}$$

Finally, the concentration C_{out} of the outgoing fluid can be estimated by a global balance, if transfer time and dispersion along the channel are neglected. In dimensional terms

$$\frac{C_{\text{out}}}{c_0} = \frac{D_{m,o}}{F_s} \frac{L_c}{Q} J. \tag{39}$$

With the values $D_{m,o} = 3.8\ 10^{-10}$ m^2/s, $1/F_s = 0.0132$, $L_c = 76\ 10^{-3}$ m, and $Q = 1.044$ mL/h, this yields

$$\frac{C_{\text{out}}}{c_0} = 1.31\ 10^{-3} J. \tag{40}$$

Numerical implementation

The experiment was simulated using a multiphase reservoir simulator capable of handling reservoir cases, with complex well operations, complex geometries, and so on. In addition, the results from the simulations were verified using a relatively simple one-phase simulator customized for the simulation of the experimental problem.

In the first case, the transport equations are discretized using a finite volume formulation using corner-point blocks. Pressure and saturation fields are obtained for each block from a host reservoir simulator, using an implicit saturation, explicit pressure (IMPES) formulation of the three-phase flow equations. The grid used to solve the concentration equations is given by the corner-point blocks of the host simulator, and the concentrations are defined in the barycenter of the reservoir blocks. A control volume, Ω, around a node in the concentration grid can be defined corresponding to the reservoir blocks surrounding this node. Gradients are represented by central differences, and concentrations are represented in the center of the discretization volume, except in the convective terms, where concentrations and saturations are represented by upstream values. The code has options for explicit and implicit solutions, but in the following simulations the implicit formulation was used. The corner-point grid used in the simulations was cylindrical, with $N_r = 72$, $N_z = 10$, and N_θ

$= 1$, which is advantageous to exploit the radial symmetry to reduce computational effort. To avoid complications posed by the innermost blocks ($r = 0$) when $N_\theta \geq 1$, an infinitesimal innermost block is defined and considered inactive.

In the one-phase numerical code, the system geometry was discretized into elementary cubic volume elements entirely filled with either sandstone, packing, or impervious confining material. The velocity field is here a constant vector aligned with the x-axis, whose magnitude is deduced from the global flow rate and the channel cross-section area. In this formulation the pressure and saturation fields are assumed constant. The solute concentration c' is determined at discrete points located at the vertices of the elementary cubes. The transport equations are discretized in a finite volume formulation, with a cubic control volume Ω of size δ^3 defined around each grid point, with the same representation for gradients and concentrations as in the first case. Finally, a first-order fully implicit scheme is applied to describe the temporal evolution of the concentration field.

Results and Discussion

Experimental results

The concentrations of phenol, *m*-cresol, *o*-cresol, and *p*-cresol in the sampled fluid from the experiment are plotted as functions of time in Figure 3. In the linear representation in Figure 3a they seem to decrease rapidly for the first 20 h, and reach quasi-constant levels for longer times. However, the logarithmic representation in Figure 3b shows a decrease even for long times. Moreover, the concentration data are proportional to the initial concentration, c_0, and collapses onto a single curve if C is normalized by c_0. This means that the solubility in water plays a negligible role, solute production from the oil is controlled by the diffusive transfer in the sandstone toward the channel.

The data collapse is a direct consequence of some of the characteristics of the experimental setup and can be analyzed with the help of the analytical model and Eq. 39. Fast solute removal, that is, the approximation (Eq. 27), is valid only as long as C_{out} is small compared to c_0/k. This means

$$k\frac{C_{\text{out}}}{c_0} = k\frac{D_{m,o}}{F_s}\frac{L_c}{Q}J \ll 1. \tag{41}$$

With the current parameters, this condition is always fulfilled due to Eq. 40. However, with a length L_c of 10 m, which might be closer to field conditions, and in a time interval $0.1 \leq t' \leq 10$ ($10 \sim 1{,}000$ h), where J is of order 1 (see Eq. 38), $k\, C_{\text{out}}/c_0$ is about $0.2k$. This means that water is nearly saturated in the least soluble organic species (*o*-cresol, $k = 3.8$) when it flows along the downstream part of the sandstone. Similarly, if the channel is filled with a less permeable material, for example, the same sandstone as the sample, and the pressure drop is kept constant, the flow rate Q will decrease dramatically, which will also induce an increase in C_{out} in the same proportion.

Considering that the dimensionless flux, J, is almost always of order one (with a time scale that depends only on the channel radius a and on the reservoir rock characteristics,

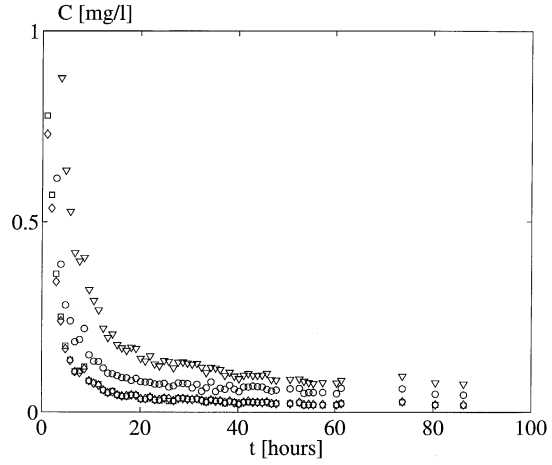

(a)

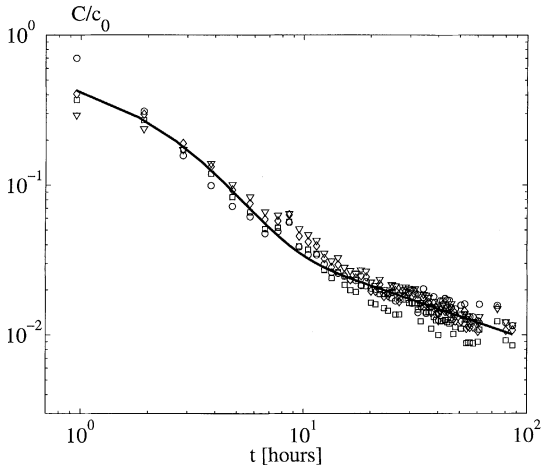

(b)

Figure 3. (a) Measured concentrations in the produced fluid in absolute value vs. time in linear scale, and (b) concentrations normalized by the initial concentration in oil c_0 in logarithmic scale.

The full line in (b) is the sum of the exponential and power-law fits defined in Eq. 43. Symbols correspond to phenol (○), *m*-cresol (□), *o*-cresol (◇), and *p*-cresol (∇).

see Eq. 20) a criterion for the diffusion limited regime is

$$k\frac{D_{m,o}}{F_s}\frac{L_c}{Q} \ll 1. \tag{42}$$

The experimental data can be represented by a sum of two functions of time

$$C/c_0 = C_1(t) + C_2(t), \qquad C_1 = 0.526\ e^{-t/T} \quad \text{with } T = 1.98 \text{ h},$$
$$C_2 = 0.0997\ t^{-0.514}, \tag{43}$$

given as a full line in Figure 3b. The power-law part, C_2, is of the form (Eq. 38) and prevails at late times. It was obtained from a least-square fit of the data for $t \geq 15$ h. The exponential part, C_1, dominates at early times, and results from a fit of $C/c_0 - C_2$ for $t \leq 7$ h.

Comparison to analytical and numerical models

In the models, the initial condition (Eq. 23) is inconsistent with the hypothesis of local equilibrium (Eq. 7). Therefore, the initial saturations were modified by a small arbitrary value $\delta_s = 10^{-4}$

$$S_w(r,x) = 1 - S_o(r,x) = \begin{cases} \delta_s & \text{if } r > a \\ 1 - \delta_s & \text{if } r \le a \end{cases} \tag{44}$$

in the two-phase numerical model, and in the one-phase model the concentration at the interfacial grid points was arbitrarily set to $c' = 1$.

An average concentration based on a global mass balance

$$C_{\text{out}} = \frac{1}{Q}\frac{d\mathfrak{M}}{dt}, \tag{45}$$

where $\mathfrak{M}(t)$ is the total amount of solute in the whole system at time t, was used to compare measured and simulated concentrations. An alternative definition based on the amount $\mathfrak{M}_s(t)$ of solute in the sandstone only, and directly comparable to the analytical prediction (Eq. 39), is

$$C_{\text{out},s} = \frac{1}{Q}\frac{d\mathfrak{M}_s}{dt}. \tag{46}$$

Normalized concentrations C_{out}/c_o and $C_{\text{out},s}/c_o$ obtained with the numerical codes and the analytical model are compared for phenol in Figure 4. For small times C_{out}/c_o obtained with the two numerical models yield different results, due to differences in the initial condition. The clear peak in the result obtained with the one-phase code is due to the solute in the initially saturated peripheral region of the packing, and occur at about 2 h, corresponding to the mean travel time to the outlet. Since the packing is excluded from the definition of $C_{\text{out},s}/c_0$, the artifact due to the initial condition is not important in this case, and the curves for $C_{\text{out},s}/c_0$ are close together from the beginning on. They join the curves for C_{out}/c_0 for $t > 10$ h, simply because the two hour time shift becomes small compared to t.

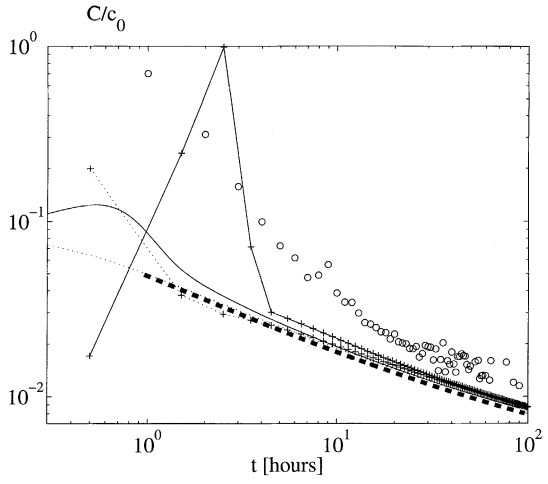

Figure 4. Concentration of phenol in the produced fluid, normalized by the initial concentration in oil c_0, vs. time in hours.

Experimental data (○) are compared to the results of C_{out} (full lines) and $C_{\text{out},s}$ (dotted lines) from the two numerical implementations of the model assuming one-phase flow. One of these implementations (—) and (· · ·) is a two-phase code where the oil has been immobilized, whereas the other (– + –) and (·· + ··) is the implementation of the one-phase model (Eqs. 13–15). The heavy broken line corresponds to the analytical solution (Eq. 39).

The excellent agreement between the numerical data and the prediction (Eq. 40) for $C_{\text{out},s}/c_0$ of the analytical model is due to the fact that the partition coefficient plays a negligible role under the experimental conditions studied here. The production of solute is controlled by the diffusive transfer in the sandstone, and subsequent transport in the sphere packing is fast enough to consider that the solute removal is quasi-instantaneous. This fast solute removal is precisely the simplifying assumption necessary for the analytical derivation.

If we compare the models to experimental results for times $t \ge 15$ h, they underestimate the measurements by about 25%, which may be explained by the error of $D_{m,o}$ and $1/F_s$, which are about 20% and 8%, respectively. Much larger discrepancies are observed at earlier times, partly due to the initial conditions discussed previously.

In addition to initial conditions, another possible source of disagreement is the use of an effective transport coefficient in a continuous transport equation for the sandstone in the close vicinity of the interface $r = a$. For instance, diffusion from the pores in the sandstone that intersect the surface $r = a$ is governed by the molecular coefficient $D_{m,o}$ multiplied by the fractional open area $\epsilon_s = 0.193$, rather than by the conductivity coefficient $1/F_s = 0.0132$.

Moreover, the plastic particles are likely to be oil wet, which may cause some oil to be trapped in the sphere packing, with a subsequent release of organic solute at a much faster rate than the oil in the sandstone sample, due to a larger specific exchange area. Small oil droplets might even be carried away by the water flow, which would explain a few values of the concentration that exceed the equilibrium saturation c_0/k. If T in Eq. 43 is equated to the time scale $r^2/D_{m,o}$ for the solute release from an oil droplet with radius r, it yields $r \approx 1.6$ mm, which is consistent with the expected size of pendular rings in a 5-mm sphere packing.

However, oil trapping, underestimated transport coefficients, and initial conditions cannot explain all the differences at early times between the numerical and experimental concentrations. Integrating C_1 in Eq. 43 over time yields a cumulated release of solute $0.526\ QTc_0$, which corresponds to a volume of oil close to 1 cm^3. This is larger than the total pore volume in the sphere packing $\epsilon_p \pi a^2 L_c \approx 0.85$ cm^3.

This suggests that oil production from the sandstone resulting from spontaneous imbibition of water is important. The sandstone was cleaned of oil and washed prior to the experiment, which tends to turn the sandstone sample from oil-wet to water-wet. If the sandstone is strongly water-wet, spontaneous imbibition can result in large oil production from the sandstone. Bourbiaux and Kalaydjian (1990), for example, find that as much as 30% of the oil is produced by spontaneous imbibition of water into a water-wet sandstone filled with oil. However, in the experiment studied by Bourbiaux

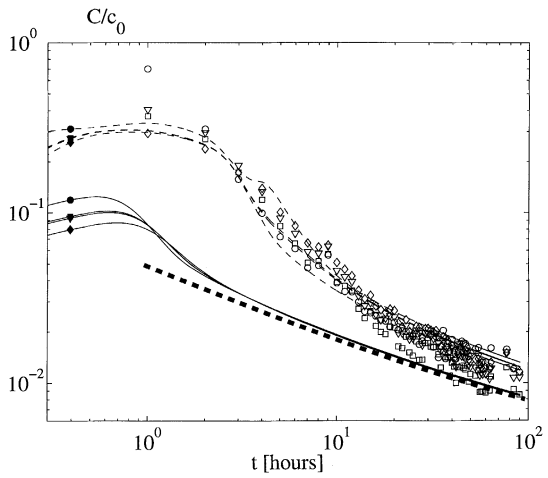

Figure 5. Concentrations in the produced fluid normalized by the initial concentration in oil c_0 vs. time in hours.

Symbols correspond to phenol (○), *m*-cresol (□), *o*-cresol (◇), and *p*-cresol (∇). Data are from the experimental measurements (open symbols) or from the numerical simulation using the two-phase code according to Eq. 45. For each solute, the model assuming immobile oil (—) is compared to the model where imbibition is considered (– – –). The heavy broken line corresponds to the analytical solution (Eq. 39).

and Kalaydjian (1990), special care was taken to ensure a strongly water-wet system. Moreover, in their case, imbibition was aided by gravity, which was not the case in our experimental setup. Therefore, 1 cm^3 of oil estimated from the integration of C_1 in Eq. 43, which corresponds to about 6.5% of oil in the sandstone, is probably a more realistic volume in our case.

Results obtained with the second model, which includes imbibition, are displayed in Figure 5 for all four solutes, and compared to the experimental data and the first model. The figure shows that when imbibition is accounted for, concentrations change significantly. For early times ($t < 15$) the curves for C_{out} are increased by a factor of about 5 with respect to C_{out} when imbibition is neglected. For long times, $t > 50$ h, C_{out} increases by about 50% if imbibition is considered. The increase for short times is expected, and illustrates precisely the assumed effect that solute is transported from the sandstone together with the oil displaced by imbibing water. For $t > 25$, very small amounts of oil are produced, and the 50% increase in C_{out} for longer times must be due to enhanced diffusion. In the model, water displaces oil in the range $a < r < d$, and after 25 h, water and oil saturations reach 90% and 10%, respectively. Diffusion coefficients in water are about two times larger than in oil, and the increase in water saturation to 90% therefore yields an enhanced diffusive transport of the solutes in this range, compared to the case without imbibition.

A collapse of data for the various solutes onto a single curve, due to the normalization of C_{out} by C_0, is apparent in the numerical results, and also in the experimental data, as noted before (see Figure 3). For long times, however, a small difference between the solutes persists, with an ordering that corresponds to the solubility in water. C/c_0 for phenol ($k = 0.3$) is the largest, followed by *m*-cresol ($k = 2.1$), *p*-cresol ($k = 2.3$), *o*-cresol ($k = 3.8$), which is consistent with the larger diffusion coefficient in water compared to oil. However, this trend is not clear in the experimental data. Further improvement of the two-phase simulation was not pursued, since it would require detailed knowledge of the permeability, wettability, and relative permeability of the sample.

Concluding Remarks

Production of four oil–water partitioning oil components, with different partition coefficients, acting as natural tracers, has been studied experimentally and analyzed with the help of analytical and numerical models. This study is a first step toward a methodology for estimating the location and size of bypassed and stagnant oil in hydrocarbon reservoirs, and NAPL contamination in subsurface water reservoirs.

In the experimental case studied here, diffusion coefficients were the most important parameters controlling the transport, and the effect of partitioning could be accounted for by a simple normalization. However, for other conditions, for example, conditions closer to reservoir conditions, partition coefficients are likely to play a more important role.

As a first approximation, the experimental results are fairly well described by a simple two-dimensional analytical model, assuming instantaneous removal of solutes from the oil–water interface. The analytical model gives a simple relation between the solute concentration in the produced water, size of the oil–water interface, diffusion coefficients, and flow rate. In cases where flow rate, diffusion coefficients and solute concentrations are known, the analytical model may therefore provide an estimate of the size of the oil–water interface, and thereby an estimate of the size of the stagnant oil or NAPL zone.

A model excluding two-phase flow effects yields results in excellent agreement with the analytical results, but underestimates the experimental results by about 25%. A two-phase model where imbibition effects are accounted for, yields a better match to the experimental data, but includes an arbitrary relative permeability curve.

It would be interesting to extend this investigation to other cases, in particular, to cases not entirely dominated by diffusion. This could be done by increasing the sample length or by decreasing the flow rate.

Finally, the investigation presented here represents the first step toward a reservoir-scale application of the methodology. The methodology developed here, including the verification and successful use of a complete reservoir simulator, shows that field-scale simulation of natural tracer transport is possible. Such field-scale simulations are in progress and will be presented in the future.

Acknowledgments

Partial funding by the European Commission under THERMIE contract OG/0277/98 is gratefully acknowledged. One of the authors (O.H.) thanks the Research Council of Norway for financial support. We thank Kimberley J. Noke for performing analytical determinations. C. Chazichristos and R. Kleven are thanked for valuable discussions.

Literature Cited

Adler, P. M., *Porous Media: Geometry and Transports*, Butterworth-Heinemann, Stoneham, MA (1992).

Aziz, K., and A. Settari, *Petroleum Reservoir Simulation*, Applied Science Publishers, London (1979).
Bear, J., *Dynamics of Fluids in Porous Media*, Dover, New York (1972).
Bennett, B., B. F. J. Bowler, and S. R. Larter, "Determination of C0-C3-Alkylphenols in Crude Oils and Waters," *Anal. Chem*., **68**, 3697 (1996).
Bennett, B., and S. R. Larter, "Partition Behaviour of Alkylphenols in Crude Oil/Brine Systems Under Subsurface Conditions," *Geochim. Cosmochim. Acta*., **61**, 4393 (1997).
Berryman, J. G., "Random Close Packing of Hard Spheres and Disks," *Phys. Rev. A*, **27**, 1053 (1983).
Bourbiaux, B. J., and F. J. Kalaydjian, "Experimental Study of Cocurrent and Countercurrent Flows in Natural Porous Media," *SPE Reservoir Eng*., **5**, 361 (1990).
Burger, J. E., G. S. Springate, and K. K. Mohanty, "Experiments on Bypassing During Gasfloods in Heterogeneous Porous Media," *SPE Reservoir Eng*., **11**, 109 (1996).
Burger, J. E., and K. K. Mohanty, "Mass Transfer from Bypassed Zones During Gas Injection," *SPE Reservoir Eng*., **12**, 124 (1997).
Carslaw, H. S., and J. C. Jaeger, *Conduction of Heat in Solids*, Oxford Univ. Press, Oxford (1959).
Coelho, D., J.-F. Thovert, and P. M. Adler, "Geometrical and Transport Properties of Random Packings of Spheres and Aspherical Particles," *Phys. Rev. E*, **55**, 1959 (1997).
Jin, M., M. Delshad, V. Dwarakanath, D. C. McKinney, G. A. Pope, K. Sepehroori, and C. E. Tilburg, "Partitioning Tracer Test for Detection, Estimation and Remediation Performance Assessment of Subsurface Nonaqueous Phase Liquids," *Water Resour. Res*., **31**, 1201 (1995).
Khachikian, C., and T. C. Harmon, "Nonaqueous Phase Liquid Dissolution in Porous Media: Current State of Knowledge and Research Needs," *Transp. Porous Media*, **38**, 3 (2000).
Le Romancer, J.-F. X., D. F. Defives, and G. Fernandes, "Mechanism of Oil Recovery by Gas Diffusion in Fractured Reservoirs in Presence of Water," *Proc. 1994 SPE/DOE Symp. on Improved Oil Recovery*, Tulsa, OK (1994).
Lichtenberger, G. J., "Field Applications of Interwell Tracers for Reservoir Characterization of Enhanced Oil Recovery Pilot Areas," *Proc. SPE Production Operations Symp*., Oklahoma City, OK (1991).
Montgomery, L. S., J. R. Wood, and W. B. Harrison, "Devonian Dundee Formation, Crystal Field, Michigan Basin: Recovery of Bypassed Oil Through Horizontal Drilling," *AAPG Bull*., **82**, 1445 (1998).
Nieminen, E., and P. Heikkila, "Simultaneous Determination of Phenol, Cresols and Xylenols in Workplace Air, Using a Polystyrene-Divinylbenzene Column and Electrochemical Detection," *J. Chromatogr*., **360**, 271 (1986).
Perry, R. H., D. W. Green, and J. O. Maloney, *Perry's Chemical Engineers' Handbook*, 7th ed., McGraw-Hill, New York (1997).
Pfannkuch, H. O., "Contribution a l'Étude des Déplacements de Fluides Micibles dans un Milieu Poreux," *Rev. Inst. Fr. Pet*., **18**, 215 (1963).
Semprini, L., O. S. Hopkins, and B. R. Tasker, "Laboratory, Field and Modelling Studies of Radon-222 as a Natural Tracer for Monitoring NAPL Contamination," *Transp. Porous Media*, **38**, 223 (2000).
Scott, G. D., "Packing of Equal Spheres," *Nature*, **188**, 908 (1960).
Taber, J. J., F. D. Martin, and R. S. Seright, "EOR Screening Criteria Revisited—Part 1: Introduction to Screening Criteria and Enhanced Recovery Field Projects," *SPE Reservoir Eng*., **12**, 189 (1997).
Walker, S., "Locating and Producing Bypassed Oil: A DOE Project Update," *Proc. 1997 SPE Western Regional Meeting*, Long Beach, CA (1997).
Watters, D. G., R. C. Maskall, I. M. Warrilow, and V. Liew, "A Sleeping Giant Awakened: Further Development of the Seria Field, Brunei Darussalam, After Almost 70 Years of Production," *Pet. Geosci*., **5**, 147 (1999).

Manuscript received Nov. 12, 2001, and revision received Oct. 30, 2002.